

Efficacy and Economic Benefits of Nano TiO₂ Photocatalytic Advanced Oxidation Technology in Solid Waste Treatment

Fan ZENG¹, Han SHI^{1*}, Xiaodong YANG¹, Wandong QIN², Zhenxun TIAN¹

¹ Hubei Three Gorges Polytechnic, No. 31, Stadium Road, Yichang City, Hubei Province, 443000, China

² Yichang Jinhui Investment Group Co., Ltd., Bailian Huigu A13-512, No. 118 Yinhe Road, Yichang City, Hubei Province, 443000, China

<http://doi.org/10.5755/j02.ms.37366>

Received 22 May 2024; accepted 4 July 2024

In order to assess the application value of nano TiO₂ photocatalytic advanced oxidation technology in the field of solid waste treatment and improve the efficiency of waste disposal, this study investigates the preparation of TiO₂/ZnIn₂S₄ composite photocatalysts using an in-situ growth method. Subsequently, this photocatalyst is applied to urban solid waste treatment schemes to degrade solid waste and organic pollutants in wastewater. The results indicate that, at a pH value of 7.5, the composite material exhibits the optimal photocatalytic degradation performance, achieving a degradation rate of 90%. Following the urban solid waste treatment scheme, the greenhouse gas emissions per ton of municipal solid waste range from 50 to 100 kg, resulting in a 90% reduction in greenhouse gas emissions. The calculated payback period for this waste treatment scheme is 5 years. The findings suggest that this treatment approach effectively reduces greenhouse gas emissions, enhances resource recovery rates, and demonstrates favorable economic benefits for application in small to medium-sized urban areas. This research provides valuable insights for the application of nano TiO₂ photocatalytic technology in the field of solid waste treatment.

Keywords: TiO₂, photocatalysis, solid waste treatment, organic pollutants, economic benefits.

1. INTRODUCTION

With the increase in population and economic development, solid waste treatment has become a global environmental challenge [1]. Solid waste refers to waste generated from various production, life, and service activities, including industrial waste, municipal garbage, agricultural waste, etc. [2]. The scale and types of these solid wastes are continuously increasing, imposing significant pressure and risks on the environment and human health [3]. Solid waste treatment involves the process of handling and disposing of solid waste, aiming to reduce its impact on the environment and human health [4]. Traditional solid waste disposal methods, such as landfilling and incineration, pose a series of issues including land resource wastage, air pollution, and soil contamination [5, 6]. Therefore, finding an efficient and environmentally friendly solid waste treatment technology is urgently needed. In recent years, photocatalytic advanced oxidation technology has gained attention as a promising solid waste treatment technique due to its advantages of non-toxicity, reliable efficiency, and absence of secondary pollution [7]. Photocatalytic advanced oxidation technology is an advanced oxidation technology that utilizes light energy to excite oxidants and combines it with light radiation. Under the action of ultraviolet light, recalcitrant organic compounds can be oxidized and decomposed, thereby achieving sewage treatment and environmental purification. Nano TiO₂ is a nanomaterial with a special structure and photocatalytic activity, capable of utilizing light energy to degrade organic and inorganic substances into harmless compounds [8]. This technology has shown great potential in areas such as water treatment,

air purification, and solid waste degradation. This study aims to enhance nano TiO₂ photocatalytic materials and analyze their application effectiveness and economic benefits in solid waste treatment, evaluating the feasibility and sustainability of nano TiO₂ photocatalytic advanced oxidation technology in solid waste treatment. The research hopes to provide valuable references for technological innovation and environmental protection in the field of solid waste treatment, promoting the widespread and practical application of nano TiO₂ photocatalytic advanced oxidation technology.

2. MATERIALS AND METHODS

2.1. Preparation of nano TiO₂ photocatalytic material

Photocatalysis is an effective method for addressing energy shortages and environmental pollution. TiO₂ is a commonly used photocatalytic material. However, it can only absorb ultraviolet light and has a low quantum efficiency [9]. TiO₂/ZnIn₂S₄ composite photocatalyst is a composite photocatalyst composed of titanium dioxide (TiO₂) and zinc indium sulfide (ZnIn₂S₄). The introduction of the co-catalyst ZnIn₂S₄ can suppress the recombination of electron-hole pairs in TiO₂, thereby enhancing the photocatalytic activity. In recent years, TiO₂/ZnIn₂S₄ composite materials have demonstrated excellent photocatalytic performance in energy and environmental applications. The study involves the in-situ growth of ZnIn₂S₄ nanoflowers on TiO₂ nanorods, resulting in the preparation of TiO₂/ZnIn₂S₄ composite photocatalysts. The

* Corresponding author. Tel.: +86-0717-8853348; fax: +86-8853338.
E-mail: shihan@tgc.edu.cn (H. San)

schematic representation of the preparation of $\text{TiO}_2/\text{ZnIn}_2\text{S}_4$ composite photocatalysts is shown in Fig. 1.

The research employed a hydrothermal reaction method to prepare rutile-type TiO_2 nanorods. Initially, 25 mL of ethylene glycol and water were measured separately using a graduated cylinder and mixed thoroughly in a dry and clean beaker. Subsequently, 20 g of NaOH particles were added to the solution, and stirring continued until complete dissolution, yielding a 10 mol/L NaOH solution. Next, 0.2 g of TiO_2 nanoparticles were added to the NaOH solution, stirred again, and then transferred to the inner vessel of a polytetrafluoroethylene container. The inner vessel with the hydrothermal reaction kettle was placed in an electric hot air-drying oven, set at 230 °C, with a reaction time of 15 hours. After the reaction, cool the outcome product to room temperature, then adjust its PH to neutral with 0.1 mol/L HCl, followed by multiple washes with water. The resulting product was then suction-filtered, and subsequent vacuum drying at 60 °C was conducted. Finally, the obtained product was placed in a crucible and placed in a horizontal vacuum crucible furnace for calcination at 500 °C under an ambient atmosphere, with a heating rate of 5 °C/min, ultimately yielding rutile-type TiO_2 nanorods.

The study involved the preparation of ZnIn_2S_4 nanoflowers through a simple water bath method. Firstly, 48 mL of H_2O and 12 mL of $\text{C}_3\text{H}_8\text{O}_3$ were placed in a clean beaker, and the pH was controlled to 2.5 with HCl (0.5 mol/L). Subsequently, 1.2 mmol of $\text{InCl}_3 \cdot 4\text{H}_2\text{O}$, 1.2 mmol of ZnCl_2 , and 3.2 mmol of $\text{C}_2\text{H}_5\text{NS}$ were individually measured and added into the solution. Then stir for 30 minutes. The solution was then transferred to a water bath at 80 °C and allowed to react for 2 hours. After the reaction, the product was centrifuged, and subsequent washing was performed with anhydrous ethanol and deionized water. Finally, the yellow precipitate was dried in

a 70 °C vacuum oven for 12 hours, resulting in the formation of ZnIn_2S_4 nanoflowers.

The research focused on the preparation of $\text{TiO}_2/\text{ZnIn}_2\text{S}_4$ composite photocatalyst materials under aquatic conditions. Initially, 48 mL of H_2O and 12 mL of $\text{C}_3\text{H}_8\text{O}_3$ were placed in a clean beaker, and the pH of the solution was adjusted to 2.5 using 0.5 mol/L HCl. Different masses (10, 30, 50, 70, 90, and 120 mg) of TiO_2 were added into the solution. Then stir for 30 minutes. Subsequently, 1.2 mmol of $\text{InCl}_3 \cdot 4\text{H}_2\text{O}$, 1.2 mmol of ZnCl_2 , and 3.2 mmol of $\text{C}_2\text{H}_5\text{NS}$ were individually measured and added to the mixed solution, followed by 30 minutes of stirring. The reaction solution was then placed in a water bath at 80 °C for 2 hours and cooled to room temperature. The reaction product was centrifuged, and multiple washes were conducted using anhydrous ethanol and deionized water. Finally, the washed product was vacuum-dried at 60 °C for 12 hours, resulting in the $\text{TiO}_2/\text{ZnIn}_2\text{S}_4$ composite photocatalyst material.

2.2. Solid waste treatment design

To address environmental issues in solid waste treatment, a solution based on $\text{TiO}_2/\text{ZnIn}_2\text{S}_4$ composite photocatalyst material is proposed. The objective is to degrade organic and inorganic components in solid waste into harmless substances, achieving effective waste treatment and resource recovery. Initially, solid waste samples are preliminarily classified and separated, distinguishing between organic and inorganic waste for separate treatment. For organic waste, exposure to a water solution containing $\text{TiO}_2/\text{ZnIn}_2\text{S}_4$ composite photocatalyst material, coupled with illumination, facilitates the degradation of organic compounds into harmless by-products such as CO_2 and H_2O .

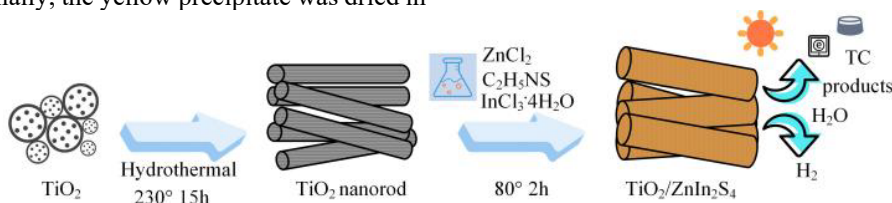


Fig. 1. Preparation schematic of $\text{TiO}_2/\text{ZnIn}_2\text{S}_4$ composite photocatalyst material

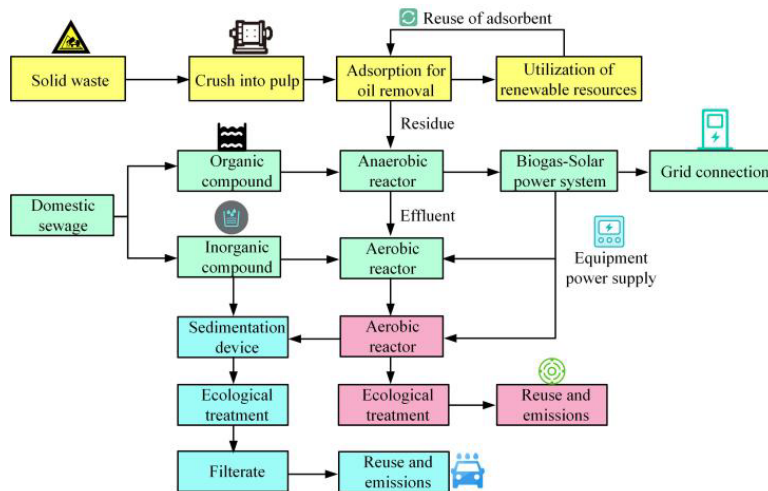


Fig. 2. Urban solid waste treatment scheme based on $\text{TiO}_2/\text{ZnIn}_2\text{S}_4$ composite photocatalyst material

In the case of inorganic waste, mixing it with the solution post-photocatalysis utilizes the photo-reductive properties of the $\text{TiO}_2/\text{ZnIn}_2\text{S}_4$ composite photocatalyst material to reduce inorganic substances into harmless metal or ion forms. During the solid waste treatment process, careful control of factors such as light conditions, catalyst dosage, and reaction time is essential to ensure the thorough degradation and conversion of waste in the photocatalytic reaction. Additionally, subsequent treatment of generated wastewater is required to prevent secondary pollution. The urban solid waste treatment scheme based on $\text{TiO}_2/\text{ZnIn}_2\text{S}_4$ composite photocatalyst material is illustrated in Fig. 2.

Urban solid waste must undergo sorting to separate recyclables, hazardous materials, and other waste [10]. Hazardous substances may include wastewater containing heavy metal ions and organic compounds. Subsequently, treatment with $\text{TiO}_2/\text{ZnIn}_2\text{S}_4$ composite photocatalyst material is employed. Initially, organic compounds and heavy metal ions in the wastewater are adsorbed onto the photocatalyst surface. TiO_2 exhibits excellent adsorption capabilities for organic compounds, while ZnIn_2S_4 can adsorb heavy metal ions. The wastewater is then subjected to precipitation treatment by adding a precipitant, allowing suspended solids and some heavy metal ions to settle, reducing the burden of subsequent processing.

Next, photocatalytic treatment is carried out. Wastewater, having undergone adsorption and precipitation treatment, is exposed to the photocatalyst under light conditions, utilizing ultraviolet light from sunlight to excite electrons and holes on the photocatalyst surface, initiating the photocatalytic reaction. During this reaction, organic compounds and heavy metal ions are degraded or transformed into harmless substances [11, 12]. The treated wastewater is filtered to remove remaining suspended solids and photocatalyst particles, resulting in clear water quality. Finally, based on the nature of the treated wastewater and the effectiveness of the treatment, it can either be reused or safely discharged. Further treatment and purification may be applied to meet reuse standards, such as for irrigation or flushing. If the treated wastewater cannot meet reuse standards, appropriate measures are taken to ensure safe discharge, avoiding environmental pollution.

2.3. Analysis methods for solid waste treatment effect and economic benefits

The assessment of the solid waste treatment effect is a crucial indicator of the success of a solid waste treatment project. To comprehensively evaluate the treatment effect of solid waste, several aspects need to be considered:

1. Waste Treatment Efficiency: This involves assessing indicators such as the waste treatment capacity, processing speed, and waste removal rate of the treatment system to measure its effectiveness. These indicators reflect the system's ability to efficiently treat waste and also demonstrate the economic and environmental aspects of the treatment process. Degradation efficiency is an important indicator for measuring the effectiveness of photocatalytic degradation, usually represented by the quality changes of pollutants before and after degradation. The efficiency of photocatalytic degradation of organic pollutants is represented by Eq. 1. In Eq. 1, the degradation efficiency is

denoted as η , and the weights of pollutants before and after photocatalytic degradation are represented by $Before_{weight}$ and $After_{weight}$, respectively.

$$\eta = \frac{Before_{weight} - After_{weight}}{Before_{weight}} \times 100\% . \quad (1)$$

2. Reduction of Environmental Impact: this aspect involves evaluating the extent to which the treatment system impacts the environment, including waste emissions, pollutant removal, and environmental restoration, to measure the system's contribution to environmental preservation. These indicators reflect the system's environmental impact and assess its environmental performance.

3. Resource Recycling: this involves evaluating the recycling rate of recyclable materials and the resource utilization efficiency of the treatment system to measure its efficiency in resource utilization. These indicators reflect the system's effective use of resources and provide an assessment of its resource utilization efficiency.

The economic benefits analysis methods for solid waste treatment mainly include cost-benefit analysis and investment payback period evaluation. Cost-benefit analysis is used for assessing the project's economic benefits by judging the costs and benefits of the treatment system. Costs include construction investment, operational maintenance costs, and human resource costs, while benefits encompass waste treatment fees, income from the sale of recyclable materials, and energy-saving and emission reduction benefits resulting from reduced carbon emissions. Investment payback period evaluation assesses the time it takes for the project to recover its investment, usually calculated on an annual basis and considering the time value of cash flow. Through these economic analysis methods, a comprehensive evaluation of the economic benefits of solid waste treatment projects can be conducted, providing valuable insights for project implementation. The methods for analyzing solid waste treatment effects and economic benefits are illustrated in Fig. 3.



Fig. 3. Analysis methods for the effectiveness and economic benefits of solid waste treatment

3. RESULTS AND DISCUSSION

3.1. The appearance of nano TiO_2 photocatalytic materials

Scanning Electron Microscopy (SEM) is a sophisticated microscopy technique in which high-energy electron beams scan the sample surface, generating secondary or backscattered electrons and producing images of the sample's morphology and microstructure. By observing these images, the morphology, size, surface characteristics, and microstructural features of the sample can be understood, enabling the evaluation and analysis of its

properties and performance. The SEM images of relevant raw materials and photocatalyst products are depicted in Fig. 4. In Fig. 4 a, the SEM image of TiO₂ nanorods demonstrates a relatively consistent diameter. The shape of TiO₂ nanorods is also generally similar, displaying a uniform nanorod structure. Additionally, the nanorod surface is smooth and exposes the (101) crystal facet. This smooth surface characteristic has a positive impact on the modification of TiO₂ nanorods. In Fig. 4 b, the SEM image of pure ZnIn₂S₄ nanosheets reveals the microstructure of densely packed nanosheets. Underwater bath conditions, numerous irregularly shaped nanosheets accumulate to form dense nanospheres with a size of approximately 2 μm. The SEM images clearly show the morphology and arrangement of these nanosheets. The irregular shape of these nanosheets may be attributed to the unique conditions during their crystal structure formation and growth process. In Fig. 4 c, the uniformly and densely coated ZnIn₂S₄ nanoflowers encapsulating TiO₂ nanorods successfully form the TiO₂/ZnIn₂S₄ heterostructure. The SEM images of TiO₂/ZnIn₂S₄ clearly illustrate the in-situ growth of ZnIn₂S₄ nanoflowers on the (101) surface of TiO₂ nanorods. This successful modification can be attributed to the minimal impact of TiO₂ surface charges on the in-situ growth process of ZnIn₂S₄ nanoflowers, allowing for close contact between the two materials and the formation of a heterojunction interface structure.

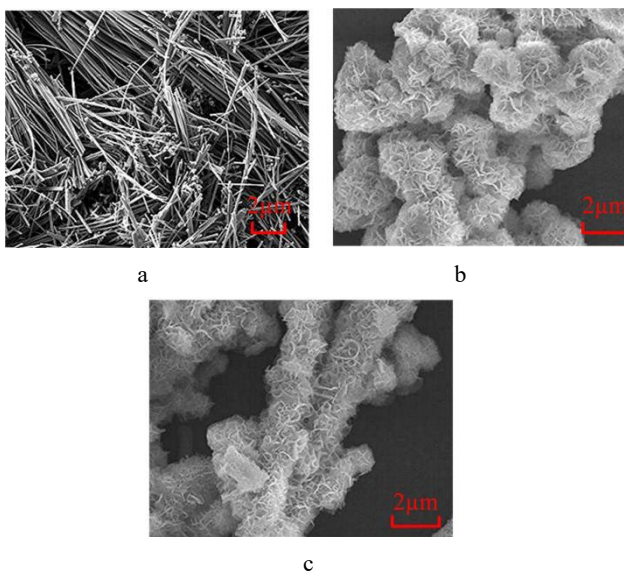


Fig. 4. SEM images of relevant raw materials and finished photocatalysts: a – TiO₂; b – ZnIn₂S₄; c – TiO₂/ZnIn₂S₄

The X-ray Diffraction (XRD) patterns of relevant raw materials and photocatalyst products are shown in Fig. 5. For TiO₂ nanorods, the XRD spectrum matches the standard rutile phase, confirming the successful preparation of rutile-type TiO₂ nanorods. In the spectrum, characteristic peaks are observed at 25.3°, 37.7°, 48.1°, 55.1°, 62.5°, 70.2°, and 75.2° for TiO₂ nanorods, with no observation of other characteristic peaks, which means evidence of the TiO₂ nanorods' high purity. For pure ZnIn₂S₄ nanoflowers, the XRD spectrum displays characteristic peaks at 20.7°, 27.4°, and 47.2°, matching the standard ZnIn₂S₄ nanoflower phase. Similarly, no other characteristic peaks are identified, confirming evidence of the ZnIn₂S₄ nanoflowers' high

purity. The XRD pattern of the TiO₂/ZnIn₂S₄ composite material closely resembles that of ZnIn₂S₄ crystals. Due to the overlap of peaks from TiO₂ nanorods and ZnIn₂S₄ nanoflowers, no distinct characteristic peaks of TiO₂ nanorods are observed. The intensity of ZnIn₂S₄ characteristic peaks in the TiO₂/ZnIn₂S₄ composite material is slightly reduced, possibly due to the addition of TiO₂ nanorods. In summary, this experiment successfully combined TiO₂ nanorods with ZnIn₂S₄ nanoflowers, resulting in the preparation of TiO₂/ZnIn₂S₄ heterojunction composite material.

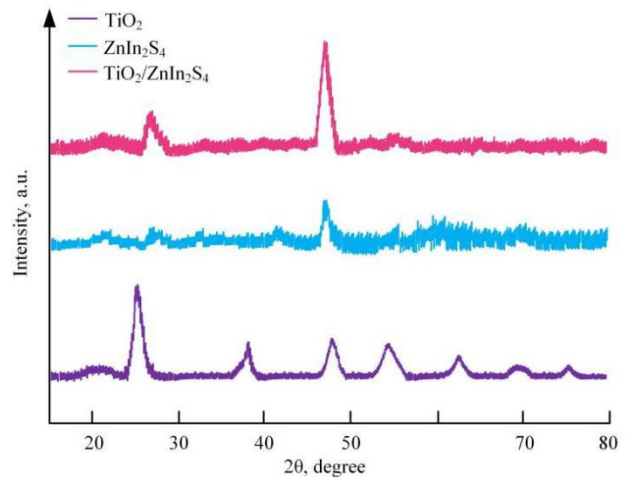


Fig. 5. XRD patterns of relevant raw materials and finished photocatalyst products

3.2. Elemental analysis of nano TiO₂ photocatalytic material

Energy-dispersive X-ray spectroscopy (EDX) is an analytical technique used to determine the elemental composition and concentration of substances. The EDX spectrum of TiO₂/ZnIn₂S₄ composite material is illustrated in Fig. 6. The EDX spectrum of the TiO₂/ZnIn₂S₄ composite material reveals a uniform distribution of Ti, O, Zn, In, and S elements within the material.

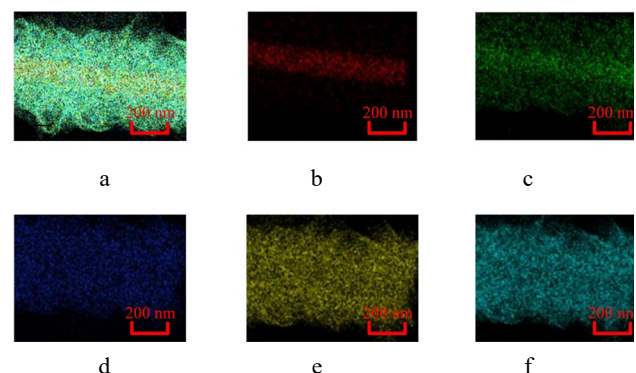


Fig. 6. EDX image of TiO₂/ZnIn₂S₄ composite material: a – EDX image of TiO₂/ZnIn₂S₄; b – EDX image of Ti in TiO₂/ZnIn₂S₄; c – EDX image of O in TiO₂/ZnIn₂S₄; d – EDX image of Zn in TiO₂/ZnIn₂S₄; e – EDX image of In in TiO₂/ZnIn₂S₄; f – EDX image of S in TiO₂/ZnIn₂S₄

By examining the elemental mapping images of Ti and O, it can be observed that they form identical nanorod-shaped TiO₂ structures. Meanwhile, Zn, In, and S elements uniformly cover the surface of the TiO₂ nanorods, indicating

the successful uniform growth of ZnIn_2S_4 nanosheets on the TiO_2 nanorods. Therefore, the $\text{TiO}_2/\text{ZnIn}_2\text{S}_4$ composite material prepared in this experiment exhibits excellent morphology. EDX determines the types and concentrations of elements in a sample by analyzing the characteristic X-rays produced after the sample is excited by X-rays. The EDX and elemental content analysis of the $\text{TiO}_2/\text{ZnIn}_2\text{S}_4$ composite material are presented in Fig. 7. In Fig. 7 a, Ti, O, Zn, In, and S elements are identified in the composite material. Detailed EDX analysis results reveal that, in terms of weight percentage in $\text{TiO}_2/\text{ZnIn}_2\text{S}_4$, the content of Ti is 12.04 %, O is 20.59 %, Zn is 15.04 %, In is 33.29 %, and S is 19.04 %. In terms of atomic percentage in $\text{TiO}_2/\text{ZnIn}_2\text{S}_4$, Ti is 9.49 %, O is 48.55 %, Zn is 8.66 %, In is 10.93 %, and S is 22.37 %. These results further confirm the successful construction of the $\text{TiO}_2/\text{ZnIn}_2\text{S}_4$ heterostructure.

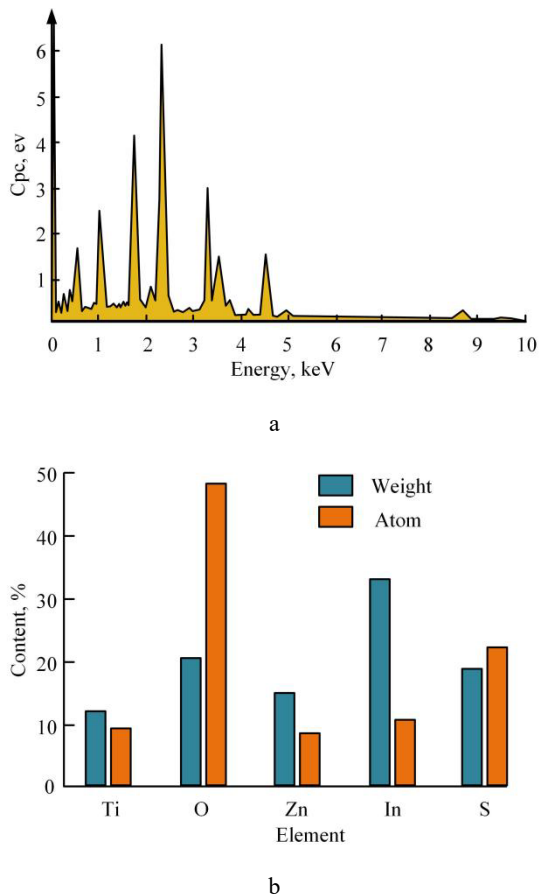


Fig. 7. a–EDS image of $\text{TiO}_2/\text{ZnIn}_2\text{S}_4$ composite material; b–elemental content analysis of $\text{TiO}_2/\text{ZnIn}_2\text{S}_4$ composite materials

3.3. Analysis of nano TiO_2 photocatalytic material properties

The fluorescence decay fitting data for the relevant raw materials and the finished photocatalyst are presented in Table 1. When compared to pure TiO_2 and ZnIn_2S_4 , it was observed that the average lifetime of photoinduced charge carriers in the $\text{TiO}_2/\text{ZnIn}_2\text{S}_4$ composite material was the longest, approximately 4.26 nanoseconds. This indicates that the heterogeneous interface structure of $\text{TiO}_2/\text{ZnIn}_2\text{S}_4$ effectively suppresses the recombination of electron-hole pairs, extending the lifetime of photoinduced charge carriers and thereby enhancing the photocatalytic performance.

Consequently, the $\text{TiO}_2/\text{ZnIn}_2\text{S}_4$ composite material exhibits a lower fluorescence decay rate, indicating a relatively slower rate of recombination of photoinduced charge carriers. This is likely attributed to the presence of the heterogeneous interface between TiO_2 and ZnIn_2S_4 , which effectively impedes the recombination process of photoinduced charge carriers.

Table 1. Fluorescence attenuation fitting data of relevant raw materials and photocatalyst finished products

Parameters	TiO_2	ZnIn_2S_4	$\text{TiO}_2/\text{ZnIn}_2\text{S}_4$
Fluorescence lifetime 1	1.31 ns	1.51 ns	1.42 ns
Pre-exponential factor 1	112.74	154.18	179.96
Fluorescence lifetime 2	5.36 ns	7.69 ns	6.48 ns
Pre-exponential factor 2	34.89	16.54	49.19
Average fluorescence lifetime	3.54 ns	3.71 ns	4.26 ns

The visible light catalytic degradation efficiency of the composite material is depicted in Fig. 8. In Fig. 8 a, the variation in the photocatalytic degradation efficiency of carbon tetrachloride by $\text{TiO}_2/\text{ZnIn}_2\text{S}_4$ composite material under different pH values is shown. At a pH of 7.5, this composite material exhibits the optimal photocatalytic degradation effect, achieving a degradation rate of 90 %. This suggests that under neutral conditions, the $\text{TiO}_2/\text{ZnIn}_2\text{S}_4$ composite material demonstrates higher photocatalytic activity against carbon tetrachloride. In Fig. 8 b, it can be observed that the $\text{TiO}_2/\text{ZnIn}_2\text{S}_4$ composite material exhibits the highest visible light photocatalytic degradation efficiency. Compared to pure TiO_2 and pure ZnIn_2S_4 , the photocatalytic degradation efficiency of the $\text{TiO}_2/\text{ZnIn}_2\text{S}_4$ composite material increased by 50 % and 30 %, respectively. This indicates that the composite of TiO_2 and ZnIn_2S_4 significantly enhances the photocatalytic activity, effectively promoting the degradation of organic pollutants.

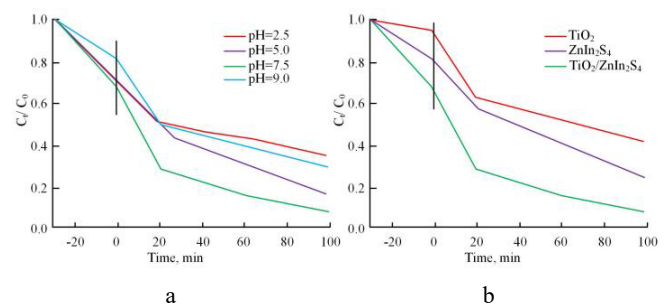


Fig. 8. Visible light catalytic degradation efficiency of composite materials: a–photocatalytic degradation efficiency and time graph of composite materials at different pH values; b–time graph of photocatalytic degradation efficiency for different samples

In conclusion, the $\text{TiO}_2/\text{ZnIn}_2\text{S}_4$ composite material demonstrates optimal photocatalytic degradation efficiency under neutral conditions (pH of 7.5), efficiently degrading organic pollutants. The notable enhancement in photocatalytic activity of this composite material compared to pure TiO_2 . In addition, the $\text{TiO}_2/\text{ZnIn}_2\text{S}_4$ composite material has a longer lifetime of photo generated charge carriers and a lower fluorescence decay rate, indicating its excellent stability and durability. The study provides an effective method for preparing efficient and stable

photocatalytic materials, which is expected to play an important role in environmental protection and energy conversion.

3.4. Analysis of solid waste treatment effect and economic benefits

To further validate the solid waste treatment effectiveness of $\text{TiO}_2/\text{ZnIn}_2\text{S}_4$ composite materials, the study investigated their application in urban solid waste treatment schemes. The removal efficiency of solid waste and the degradation efficiency of organic pollutants in photocatalytic reactions are depicted in Fig. 9. In Fig. 9 a, the solid waste content at the inlet ranged from 25 to 350 mg/L, while at the outlet, it was within the range of 25 to 100 mg/L, resulting in an overall solid waste removal rate exceeding 75 %. This indicates that the photocatalytic reaction effectively removes solid waste from wastewater. In Fig. 9 b, the chemical oxygen demand (COD) at the inlet ranged from 300 to 400 mg/L, while at the outlet, it was within the range of 20 to 100 mg/L, with the degradation efficiency of organic pollutants ranging from 85 % to 90 %. This demonstrates that the photocatalytic reaction has a high efficiency in degrading organic pollutants. In summary, the $\text{TiO}_2/\text{ZnIn}_2\text{S}_4$ composite material in the photocatalytic reaction exhibits excellent performance in the removal of solid waste and degradation of organic pollutants, providing an effective technical means for wastewater treatment.

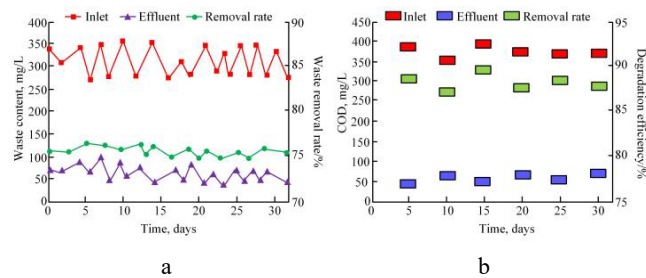


Fig. 9. a – photocatalytic reaction waste removal rate; b – organic pollutant degradation efficiency of photocatalytic reaction

The impact of the urban solid waste treatment scheme based on $\text{TiO}_2/\text{ZnIn}_2\text{S}_4$ composite photocatalyst materials on environmental and resource recovery is illustrated in Fig. 10. In Fig. 10 a, when untreated, the greenhouse gas emissions from every ton of urban solid waste range from 700 to 1000 kg.

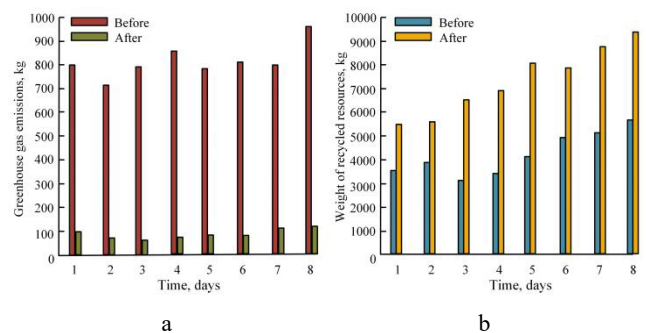


Fig. 10. The impact of urban solid waste treatment schemes on the environment and resource recovery: a – environment; b – resource recycling

After treatment by the urban solid waste treatment scheme, the greenhouse gas emissions per ton of urban solid waste are reduced to the range of 50 to 100 kg, representing a 90 % reduction in greenhouse gas emissions. In Fig. 10 b, when untreated, the daily resource recovery of urban solid waste ranges from 3000 to 5000 kg. After treatment by the urban solid waste treatment scheme, the daily resource recovery of urban solid waste is in the range of 5400 to 9500 kg, resulting in a 25 % increase in resource recovery rates. The results indicate that the urban solid waste treatment scheme not only contributes to reducing greenhouse gas emissions and mitigating environmental pollution but also effectively enhances resource recovery rates, offering an environmentally friendly and resource-efficient solution for urban solid waste treatment.

The economic analysis of solid waste treatment in the application of the urban solid waste treatment scheme in small and medium-sized cities is illustrated in Table 2. The construction investment for the solid waste treatment scheme amounts to 8 million RMB, with annual operation and maintenance costs of 1 million RMB and human resource costs also totaling 1 million RMB per year.

Table 2. Economic benefits analysis of solid waste treatment

Economic benefits	Classification	Index	Data
Cost effectiveness	Cost income cost	Construction investment	8 million yuan
		Operation and maintenance	1 million yuan/year
		Human resources	1 million yuan/year
	Income	Waste disposal	1020 yuan/ton
		Recyclable sales	950 yuan/ton
		Carbon emissions reduction	5 million yuan/year
Investment payback period	/	/	5 years

The solid waste treatment scheme generates income through solid waste treatment, the sale of recyclables, and the reduction in carbon emissions. Specifically, the income per ton from solid waste treatment is 1,020 RMB, while the revenue from the sale of recyclables amounts to 950 RMB per ton, and there is an annual income of 5 million RMB from the reduction in carbon emissions. Through calculations, it is determined that the payback period for this solid waste treatment scheme is 5 years. This indicates that within 5 years after the investment and construction, the scheme can recover the entire investment cost and begin to generate economic benefits for the city. The results indicate that this urban solid waste treatment scheme demonstrates favorable economic benefits in the context of small and medium-sized cities. The calculation of the payback period reveals that this scheme can recoup the investment costs within a relatively short timeframe and create stable economic income for the city. Furthermore, the solid waste treatment scheme can further augment income through the sale of recyclables and the reduction in carbon emissions. Hence, this scheme not only effectively addresses urban

solid waste issues but also brings considerable economic benefits to the city.

3.5. Discussion

Under light conditions, photocatalytic materials can promote the generation of electron hole pairs and utilize these electron-hole pairs for surface reactions, thereby achieving various applications such as pollutant degradation, air purification, CO₂ reduction, solar cells, antibacterial and self-cleaning. At present, common photocatalytic materials mainly include metal oxides, non-metallic semiconductors, and sulfides. TiO₂, as an excellent photocatalyst, has attracted attention due to its low cost and environmentally friendly characteristics. Researchers have continuously improved the photocatalytic efficiency of TiO₂ by changing its heterojunction morphology, size, and structure, as well as element doping, in order to solve environmental pollution problems [13]. The study successfully achieved the treatment of urban solid waste by preparing TiO₂/ZnIn₂S₄ composite photocatalyst materials. This composite material not only has excellent photocatalytic activity, but also can effectively degrade organic pollutants and solid waste, similar to the P/MoS₂ composite photocatalyst synthesized by Zhao et al. [14]. Yadav et al. prepared vanadate (V₂O₅) and V₂O₅/RGO (reduced graphene oxide) composite materials by hydrothermal method, and characterized them through various analytical methods. The results show that the V₂O₅/RGO composite material has better photocatalytic performance than V₂O₅ [15]. The TiO₂/ZnIn₂S₄ composite material exhibits the highest photocatalytic degradation efficiency of carbon tetrachloride under neutral conditions, significantly better than pure TiO₂ and pure ZnIn₂S₄, which is similar to the research results of Yadav et al. In addition, the composite material has a long lifetime of photo generated charge carriers and a low fluorescence decay rate, indicating excellent stability and durability, similar to the research results of Rasouli et al. [16]. In terms of solid waste treatment efficiency, TiO₂/ZnIn₂S₄ composite material exhibits a high solid waste removal rate and organic pollutant degradation efficiency. The results show that TiO₂/ZnIn₂S₄ composite material has significant performance advantages in photocatalytic reactions for solid waste removal and organic pollutant degradation.

The long-term stability and durability of photocatalytic materials are key factors affecting their application effectiveness in environmental protection and other fields. In order to improve the stability and durability of photocatalytic materials, research has been conducted from multiple aspects. Firstly, choose a foundation material with higher stability. Secondly, by using methods such as carrier loading and composite, the dispersion and interface properties of photocatalytic materials can be improved, thereby enhancing their stability. In addition, optimizing the preparation process of photocatalytic materials, such as controlling crystal structure and particle size distribution, can improve material quality. At the same time, surface modification methods such as stabilizers and protective layers are added to enhance the environmental stability of photocatalytic materials. However, this study still faces many challenges in improving the stability and durability of

photocatalytic materials. In the future, further in-depth research is needed in material design, preparation processes, reaction systems, and other aspects to provide more reliable photocatalytic materials for practical applications

4. CONCLUSIONS

The study aims to explore the effectiveness and economic benefits of nano TiO₂ photocatalytic advanced oxidation technology in the treatment of solid waste. TiO₂/ZnIn₂S₄ composite photocatalysts were prepared using an in-situ growth method for the treatment of urban solid waste. The results indicate that, at a pH of 7.5, the composite material exhibits optimal photocatalytic degradation, achieving a degradation rate of 90 %. After applying this urban solid waste treatment scheme, the solid waste content at the effluent ranges from 25 to 100 mg/L, with an overall waste removal rate exceeding 75 %. The effluent COD falls within the range of 20–100 mg/L, and the degradation efficiency of organic pollutants is in the range of 85 %–90 %. The greenhouse gas emissions per ton of urban solid waste are within the range of 50–100 kg, resulting in a 90 % reduction in greenhouse gas emissions. The research indicates that nano TiO₂ photocatalytic advanced oxidation technology has a significant impact on solid waste treatment, effectively degrading solid waste and organic pollutants in wastewater, reducing greenhouse gas emissions, increasing resource recovery efficiency, and demonstrating good economic benefits in the application to small and medium-sized cities. However, the limitations of this study include the need for further research and improvement in the selection and optimization of certain parameters. Future research could explore the effects of different photocatalyst dosages and reaction times on treatment outcomes to further enhance the performance of photocatalytic solid waste treatment.

Acknowledgments

We would like to express our gratitude to the editors of the journal. Their dedication and professional expertise laid the foundation for the successful publication of the article. Their diligent efforts have facilitated the smooth presentation of the article to the readers.

REFERENCES

1. Zhang, S., Chen, Z., Lin, X., Wang, F., Yan, J. Kinetics and Fusion Characteristics of Municipal Solid Waste Incineration Fly Ash During Thermal Treatment *Fuel* 279 (1) 2020: pp. 118410–118422. <https://doi.org/10.1016/j.fuel.2020.118410>
2. Hyunah, K., Hannah-Noa, B., Alex, R.S.O., Alarcón-Correa, M., Hahn, K., Richter, G., Fischer, P. Dry Synthesis of Pure and Ultrathin Nanoporous Metallic Films *ACS Applied Materials & Interfaces* 15 (4) 2023: pp. 5620–5627. <https://doi.org/10.1021/acsami.2c19584>
3. Cao, X., Zhang, L., Guo, C., Chen, T., Feng, C., Liu, Z., Qi, Y., Wang, W., Wang, J. Ni-doped CdS Porous Cubes Prepared from Prussian Blue Nanoarchitectonics with Enhanced Photocatalytic Hydrogen Evolution Performance *International Journal of Hydrogen Energy* 47 (6) 2022: pp. 3752–3761.

<https://doi.org/10.1016/j.ijhydene.2021.11.016>

4. **Belabed, C., Tab, A., Moulai, F., Cernohorsky, O., Boudiaf, S., Benrekaa, N., Grym, J.M.** ZnO Nanorods-PANI Heterojunction Dielectric, Electrochemical Properties, and Photodegradation Study of Organic Pollutant under Solar Light *International Journal of Hydrogen Energy* 46 (40) 2021: pp. 20893–20904.
<https://doi.org/10.1016/j.ijhydene.2021.03.195>
5. **Pokluda, A., Anwar, Z., Boguschová, V., Anusiewicz, I., Skurski, P., Sikorski, M., Cibulka, R.** Robust Photocatalytic Method Using Ethylene-Bridged Flavinium Salts for the Aerobic Oxidation of Unactivated Benzylic Substrates *Advanced Synthesis & Catalysis* 363 (18) 2021: pp. 4371–4379.
<https://doi.org/10.1002/adsc.202100024>
6. **Liao, G., Tao, X., Fang, B.** An Innovative Synthesis Strategy for High-efficiency and Defects-switchable-hydrogenated TiO₂ Photocatalysts *Matter* 5 (2) 2022: pp. 377–379.
<https://doi.org/10.1016/j.matt.2022.01.006>
7. **Wang, T., Chen, L., Chen, C., Huang, M., Huang, Y., Liu, S., Li, B.** Engineering Catalytic Interfaces in Cu^{δ+}/CeO₂-TiO₂ Photocatalysts for Synergistically Boosting CO₂ Reduction to Ethylene *ACS nano* 16 (2) 2022: pp. 2306–2318.
<https://doi.org/10.1021/acsnano.1c08505>
8. **Kaewkam, P., Kanchanapaetnukul, A., Khamyan, J., Phadmanee, N., Lin, K.Y.A., Kobwittaya, K., Sirivithayapakorn, S.** UV-assisted TiO₂ Photocatalytic Degradation of Virgin LDPE Films: Effect of UV-A, UV-C, and TiO₂ *Journal of Environmental Chemical Engineering* 10 (4) 2022: pp. 108131–1081448.
<https://doi.org/10.1016/j.chemosphere.2022.136163>
9. **Kocijan, M., Ćurković, L., Gonçalves, G., Podlogar, M.** The Potential of rGO@ TiO₂ Photocatalyst for the Degradation of Organic Pollutants in Water *Sustainability* 14 (19) 2022: pp. 12703–12721.
<https://doi.org/10.3390/su141912703>
10. **Qin, S., Denisov, N., Will, J., Kolařík, J., Spiecker, E., Schmuki, P.** A Few Pt Single Atoms are Responsible for the Overall Co-Catalytic Activity in Pt/TiO₂ Photocatalytic H₂ Generation *Solar RRL* 6 (6) 2022: pp. 2101026–2101032.
<https://doi.org/10.1002/solr.202101026>
11. **Zweigle, J., Bugsel, B., Capitain, C., Zwiener, C.** PhotoTOP: PFAS Precursor Characterization by UV/TiO₂ Photocatalysis *Environmental Science & Technology* 56 (22) 2022: pp. 15728–15736.
<https://doi.org/10.1021/acs.est.2c05652>
12. **Paumo, H.K., Dalhatou, S., Katata-Seru, L.M., Kamdem, B.P., Tijani, J.O., Vishwanathan, V., Abdoulaye, K., Bahadur, I.** TiO₂ Assisted Photocatalysts for Degradation of Emerging Organic Pollutants in Water and Wastewater *Journal of Molecular Liquids* 331 (2) 2021: pp. 11548–115475.
<https://doi.org/10.1016/j.molliq.2021.115458>
13. **Yang, H., Yang, B., Chen, W., Yang, J.** Preparation and Photocatalytic Activities of TiO₂-based Composite Catalysts *Catalysts* 12 (10) 2022: pp. 1263–1301.
<https://doi.org/10.3390/catal12101263>
14. **Zhao, G., Ma, W., Wang, X., Xing, Y., Hao, S., Xu, X.** Self-water-absorption-type Two-dimensional Composite Photocatalyst with High-efficiency Water Absorption and Overall Water-splitting Performance *Advanced Powder Materials* 1 (2) 2022: pp. 100008–100017.
<https://doi.org/10.1016/j.apmate.2021.09.008>
15. **Yadav, A.A., Hunge, Y.M., Kang, S.W., Fujishima, A., Terashima, C.** Enhanced Photocatalytic Degradation Activity Using the V₂O₅/RGO Composite *Nanomaterials* 13 (2) 2023: pp. 338–347.
<https://doi.org/10.3390/nano13020338>
16. **Rasouli, K., Alamdari, A., Sabbaghi, S.** Ultrasonic-assisted Synthesis of α-Fe₂O₃@TiO₂ Photocatalyst: Optimization of Effective Factors in the Fabrication of Photocatalyst and Removal of Non-biodegradable Cefixime via Response Surface Methodology-central Composite Design *Separation and Purification Technology* 307 (1) 2023: pp. 122799–122816.
<https://doi.org/10.1016/j.seppur.2022.122799>



© Zeng et al. 2024 Open Access This article is distributed under the terms of the Creative Commons Attribution 4.0 International License (<http://creativecommons.org/licenses/by/4.0/>), which permits unrestricted use, distribution, and reproduction in any medium, provided you give appropriate credit to the original author(s) and the source, provide a link to the Creative Commons license, and indicate if changes were made.